

JAN SZCZYPIOR, RAFAŁ JAKUBOWSKI*

THERMAL CALCULATIONS AND TESTING OF EXTERNAL ROTOR PERMANENT MAGNET MACHINE

OBLICZENIA I BADANIA CIEPLNE MASZyny Z MAGNESAMI TRWAŁYMI I ZEWNĘTRZNYM WIRNIKIEM

Abstract

The work concentrates on the thermal calculations and tests of the permanent magnet machine with an external rotor and cooled with liquid flowing around the inner surface of the stator frame. The distribution of the temperature in the cross-section of the machine, obtained as a result of the thermal net solutions in a steady state is presented. The calculation results are compared with the test results.

Keywords: outer rotor PM electrical machines, thermal calculations, thermal tests of electrical machines

Streszczenie

W pracy przedstawiono model do obliczeń cieplnych i stanowisko do badań maszyny z magnesami trwałymi i zewnętrznym wirnikiem, w której wewnętrzna powierzchnia korpusu stojana jest chłodzona cieczą. Zaprezentowano rozkład temperatury w przekroju poprzecznym maszyny otrzymany w wyniku rozwiązania zastępczej sieci cieplnej, w stanie ustalonym. Wyniki obliczeń porównano z wynikami badań.

Słowa kluczowe: maszyna elektryczna z magnesami trwałymi, obliczenia cieplne, badania cieplne

DOI: 10.4467/2353737XCT.15.058.3858

* Ph.D. Eng. Jan Szczypior, M.Sc. Rafał Jakubowski, Institute of Electrical Machines, Faculty of Electrical Engineering, Warsaw University of Technology.

1. Introduction

The work refers to the permanent magnet machine with an outer rotor designed for the direct drive of an electric vehicle. Knowledge of the temperature distribution inside the machine is needed for the proper design of the magnetic circuit and cooling system. Parameters of neodymium magnets worsen with the increase of temperature. Cooling systems should ensure that the maximum and average temperature in the magnets and winding are not exceeded. These temperatures are the input data for electromagnetic calculation which gives the design and operational parameter of the machine.

Vehicle requirements and the first version of the machine construction are presented in [1]. The machine has continuous power of 5 kW at a speed of 330 rev/rpm. Additionally, the machine must ensure a triple torque overload and a 70% increase of speed. The machine presented in this paper is different to the machine discussed in [1] with regard to:

- bearing system, which provides easier access and regulation of bearing slackness,
- design of disk and rotor body which allows increasing the maximum speed,
- seal system, which improves its efficiency and reliability.

Construction of the presented machine is shown in Fig. 1, a view of the built prototype is shown in Fig. 2.

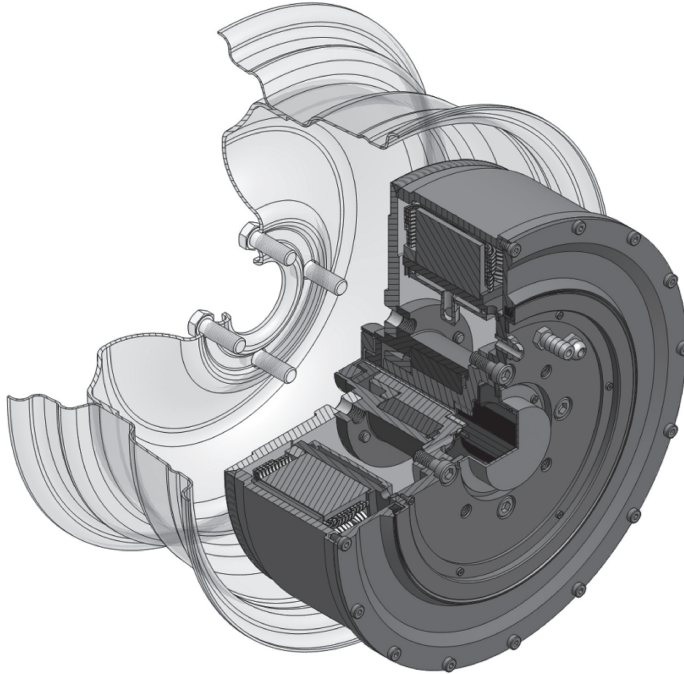


Fig. 1. Construction of machine

Thermal model of machine including stator and cooling channel is presented in [2].

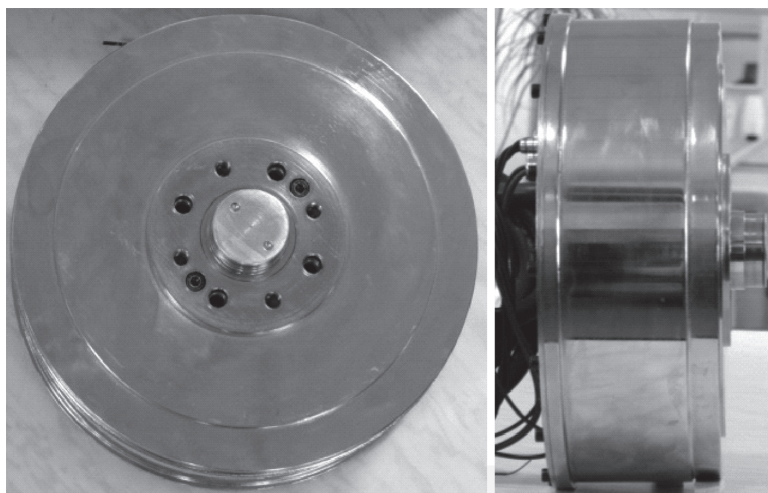


Fig. 2. View of built prototype

In this paper, two methods of cooling were compared. A cooling solution with two parallel circuits (inlet to the channel at the bottom and outlet at the top), which is considered in this work, enabled lower temperatures and easier channel venting. Initial tests of the built prototype have shown that the thermal model should also include the rotor. The reason for this is that the power losses generated were due to flux pulsation in the magnets and yoke. Moreover, rotating the outer rotor is cooled by the air. What is more, heat transfer from the stator disk to the structure which mounts it to the stand or vehicle suspension, was observed and taken into consideration.

In the following part of the paper, the thermal model of the machine and results of calculations are presented, which are then compared with measurements made on the research stand.

2. Thermal model of the machine

In order to model the temperature distribution in the machine in a thermal steady state, thermal network was used [3–6]. By ignoring differences in the temperature along the length of the machine, a two-dimensional thermal model of half machine from the inlet to the outlet of the cooling medium was built. The modelled half of the machine was divided into elementary volumes by planes RZ and $Z\Theta$. These volumes have the same thickness, which equals l_s – length of the stator packet. Elementary volumes in the teeth area have a constant width and rectangular prism shape, the remaining volumes have shape of the ring sector. The dimensions of the elementary volumes were made dependent from parameters of the design and discretization.

To the set of design parameters belong: Q_s – number of stator slots; r_{re} – outer rotor radius; h_{jr} – height of rotor yoke; h_m – magnets height; α_e – pole magnet fill factor; δ – thickness of the air gap; r_{se} – stator outer radius; h_{ds} – stator tooth height; b_d – stator tooth width; h_{js} – height of the stator yoke; d_{sp} – thickness of gap between stator and body; g_{ks} – thickness of stator body wall; h_k – height of cooling channel.

Division into the elements of the modelled area define the list of the following parameters: n_{rjs} – number of layers in stator yoke along radius; n_{rd} – numbers of layers in slot and tooth along radius; n_{rm} – number of layers in permanent magnet along radius; n_{rjw} – number of layers in rotor yoke along radius; n_{fid} – number of divisions around angle in tooth area; n_{fiq} – number of divisions around angle in slot area. Angle division parameters in slot-tooth area are passed on to remaining areas of the machine. The areas of the cooling channel with medium, stator frame, air gaps between stator packet body and air gaps between stator and rotor, was modelled as a single layer in the radial direction. Due to this, a parametric thermal model of the machine which allows easily changing the design parameters was obtained. A fragment of the thermal network from the model of half of the machine for exemplary division is shown in Fig. 3.

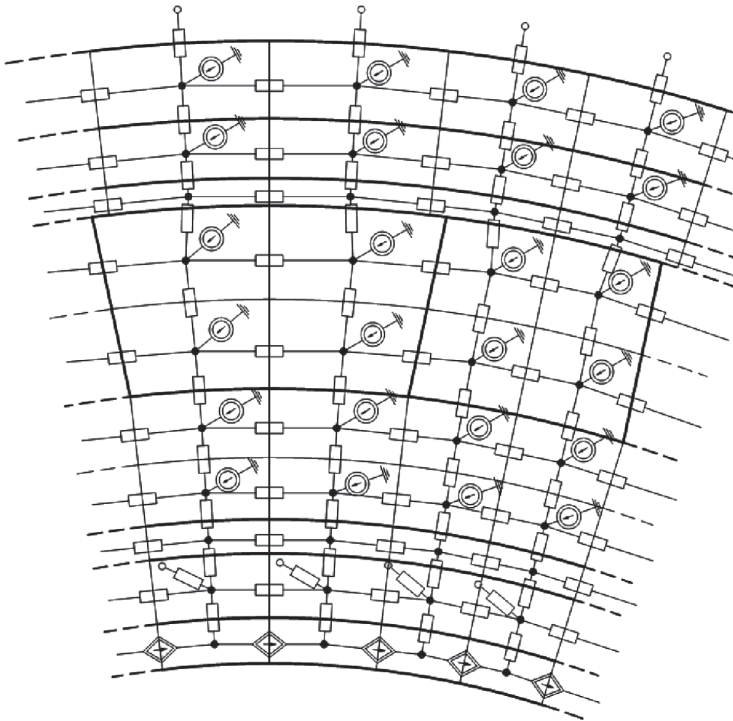


Fig. 3. Fragment of thermal network of machine

The model takes into account heat transfer to other elements and to the surroundings through conduction and convection (emission was omitted). Convection occurs during heat transfer from channel faces to the cooling medium, from stator and rotor surfaces to the air-gap, and from the rotor surface to the surrounding air. In the remaining parts of the machine, heat transfer occurs by conduction.

Power losses generated in winding, in the stator core, in the rotor core, and in the magnets are here the heat sources. Power losses in the windings were determined on the basis of winding resistance and assumed currents. Stator core losses were determined in design calculations. Rotor core losses and losses in magnets were determined based on the mechanical power of

the machine which drives the tested machine during no load test. Knowing power generated in different regions of machine, power losses emitted in elementary volumes were determined.

The set-point temperature of cold water in the model is the reference temperature. Branches in the outer layer of the rotor and stator body are connected with reference temperature. Power losses and heat fluxes in the branches connected to the reference temperatures are heat sources in the thermal network which flow into the nodes. The heat exchange in the channel was modelled as sources of heat flux controlled by temperature of liquid [3, 5].

The thermal network was solved by using a method analogous to the nodal potential method used in electrical networks. In thermal networks, potentials correspond to temperature and heat fluxes correspond to currents or power losses. According to this method, conduction and convection conductance was matched in thermal self-conductance matrix \mathbf{G} (sum of conductance attached to a given node) and mutual ones (existing between adjacent nodes). Power losses and heat fluxes in branches connected to reference temperatures \mathbf{Q} , were matched in source vector \mathbf{P} . The equation system with unknown temperatures, has the form:

$$\mathbf{G} \cdot \mathbf{Q} = \mathbf{P} \quad (1)$$

The program for building and solving the thermal model of the machine was written in Matlab. The program allows graphical visualization of results in the form of graphs and maps of temperature. A detailed description of algorithm of formulation and the solution of the thermal network is presented in [4 and 5].

3. Results of calculations

In thermal calculations presented in [2], it was assumed that the thermal conductance coefficient in the channel can range from 500 to 2000 W/m²K. The value of this coefficient depends on the geometry of the channel, liquid velocity, thermal conductivity, viscosity and liquid density. Accordingly, the value of this coefficient is often determined experimentally. In order to find the dependence α_k on the liquid velocity and temperature for three coolant flow rates 0.25, 0.5 and 1 l/minute Reynolds number was calculated [7]:

$$Re = \frac{\rho u d}{\eta} \quad (2)$$

where:

ρ – density of liquid [kg/m³],

η – coefficient of dynamic viscosity of liquid [Pa·s],

u – average linear speed [m/s],

d – equivalent diameter of channel [m], equal $4S_k/b_k - S_k$ – channel cross-section, b_k – circumference of channel.

Calculations were made for water. Density, coefficient of dynamic viscosity and conductivity of water were made conditional on temperature in the range from 10 to 60°C. The value of the Reynolds number in all cases was lower than 2100. This means that the flow is laminar. Next, the Prandtl number was calculated:

$$Pr = \frac{c\eta}{\lambda} \quad (3)$$

where:

c – specific heat [J/kg·K],

λ – thermal conductivity [W/m·K] of water, as a temperature function.

With laminar flow, the Nusselt number is determined as:

$$Nu = C(Re Pr l_k / d)^n \quad (4)$$

where l_k is channel length.

Value of C and n depend on the product value in brackets (4). Calculated values of the product were greater than 13, therefore $C = 1.86$, $n = 0.33$. Based on the Nusselt number, the heat transfer coefficient in the channel was calculated.

$$\alpha_k = \frac{C(Re Pr l_k / d)^n \lambda}{d} \quad (5)$$

Calculation results were shown in Fig. 4. The figure shows that α_k increases non-linearly depending on the liquid temperature and velocity.

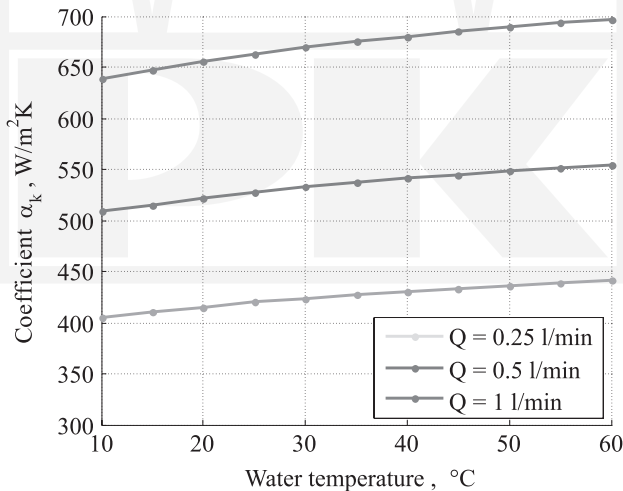


Fig. 4. Dependence of coefficient α_k on liquid temperature and discharge

Calculated values of α_k were used in thermal calculation for the same flow rate of liquid in the channel and for 1.8 times overload of the machine. This overloading was determined in such a way that the maximum temperature of the winding for the smallest liquid flow was close to 120°C. Despite a much greater allowable winding temperature (200°C), such a temperature

was adopted as the maximum due to the adverse effect of temperature on magnet parameters. For easier comparisons of calculation results with research results, the same temperature of cold water was set up (26.5°C). Results of calculations at a flow equal to 0.25 l/min is shown in Fig. 5a) and b), and at a flow equal to 0.5 and 1 l/min, in Fig. 6a) and b).

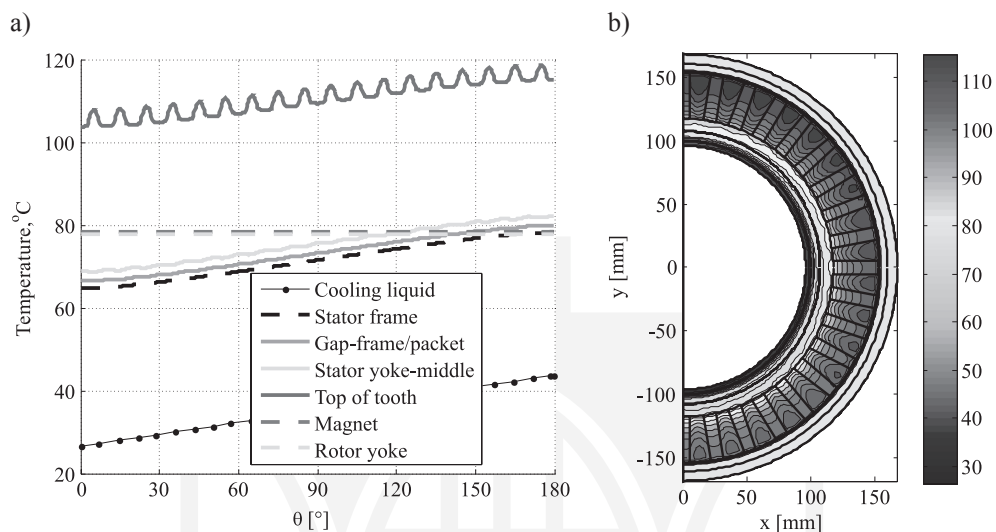


Fig. 5. Temperature distribution in: a) selected areas of constant radius and angle in the range of 0 to 180°, at a flow of liquid 0.25 l/min, b) cross-section of the machine at liquid flow 0.25 l/min

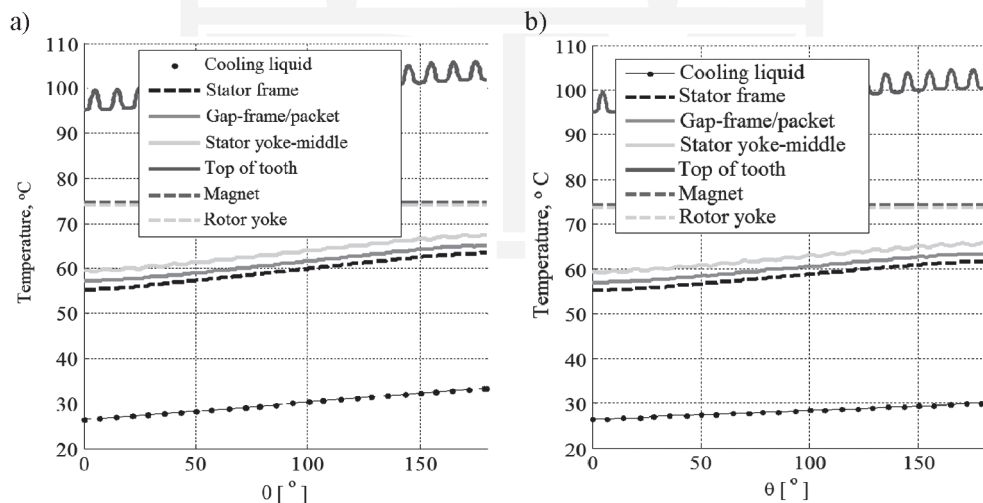


Fig. 6. Temperature distribution in selected areas of constant radius and angle in the range of 0 to 180°, at a flow of liquid: a) 0.5 l/min, b) 1 l/min

4. Machine research

Research of the built prototype was performed on the stand shown in Fig. 7a). The machine was installed in a handle and connected by a system of flexible coupling and a torque meter with a DC machine equipped with a planetary gear. The tested machine was cooled by distilled water in a closed system consisting of a pump with a regulated flow cooling channel inside the stator frame, the flowmeter and the radiator with a fan. 12 type LM135 temperature sensors was placed in the machine. The sensors were placed on two coils located closest to the inlet and outlet of liquid.

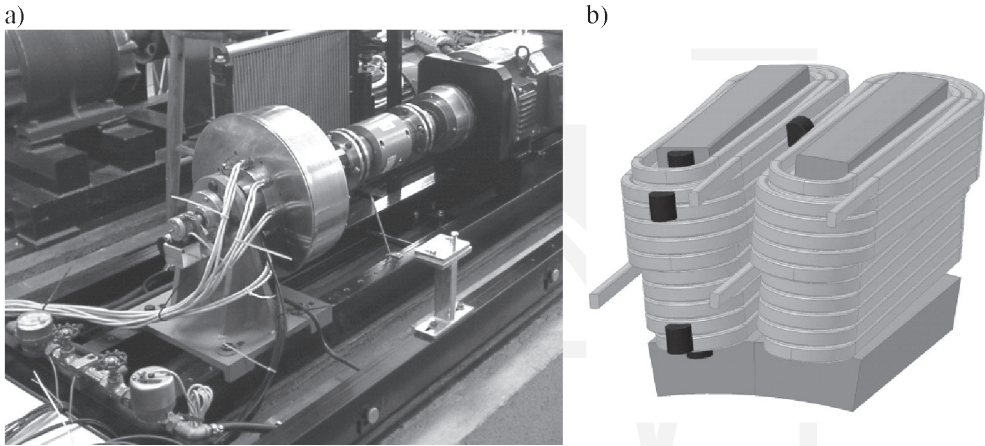


Fig. 7. a) The stand for research of the machine, b) Arrangement of temperature sensors in the coil located closest to the liquid outlet

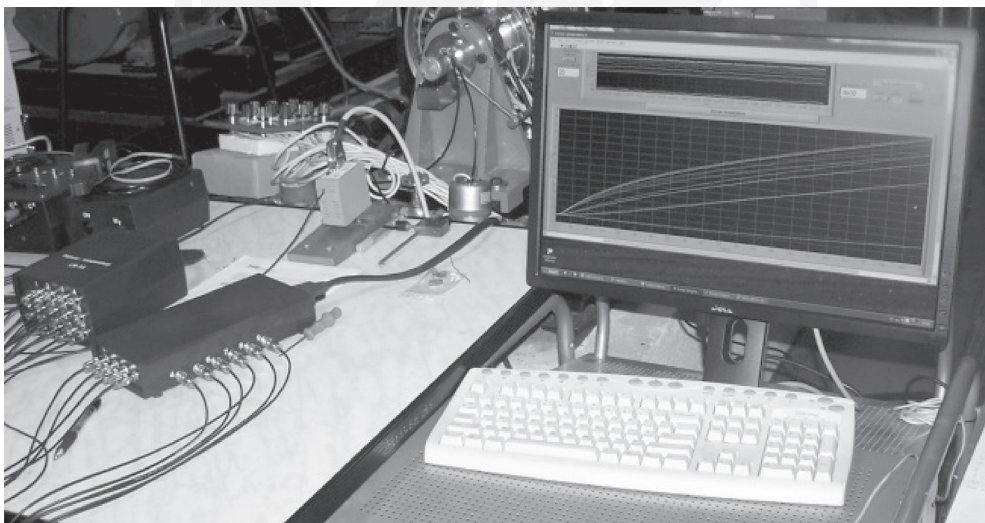


Fig. 8. System for temperature recording

Sensor arrangement in one coil area is shown in Fig. 7b). The remaining 2 sensors measured the temperature of the liquid flowing in and out of the machine.

The measured temperatures were registered using a measuring data card NI PCI 6251 connected to a computer and a specially developed virtual instrument. This device allows simultaneous recording of temperature from 12 sensors in set-up time. Signals from sensors were read at frequency 1 kHz. In order to reduce the number of data points and eliminate random noises, measurements were averaged over 1 sec. Temperature from each sensor calculated in this way was saved in the form of a file. After each results recording, in graphic window of control panel of the instrument current temperature dependence as a function of time were displayed, Fig. 8.

Research was performed in generator state of machine. The machine was driven by a DC motor and loaded with regulated resistance. Three heating tests were performed for the flow rate of liquid in channel (0.25, 0.5 and 1 l/min) and in overload (1.8), same as in the calculation. The time of each test was limited to 120 minutes. After this time, temperatures were practically steady. The maximum temperature in the winding was indicated by the sensor attached to the coil in the middle of the machine length. The maximum temperature dependences on time in the coil located at the outlet (solid lines) and the coil placed near the cooling liquid inlet (dashed line) are shown in Fig. 9. This figure shows that for liquid flow of 0.25 l/min, maximum temperature of the winding is approximately 118°C and is close to the calculated temperature shown in Fig 5a). From Figs. 9, 5a), 6a) and b) show that increases in liquid flow above 0.5 l/min cause a slight reduction in the maximum temperature of the winding. With increasing the flow from 0.5 to 1 l/min the temperature was reduced by only approx. 3°C, while the increase in the flow from 0.25 to 0.5 l/min reduced the temperature by about 10°C.

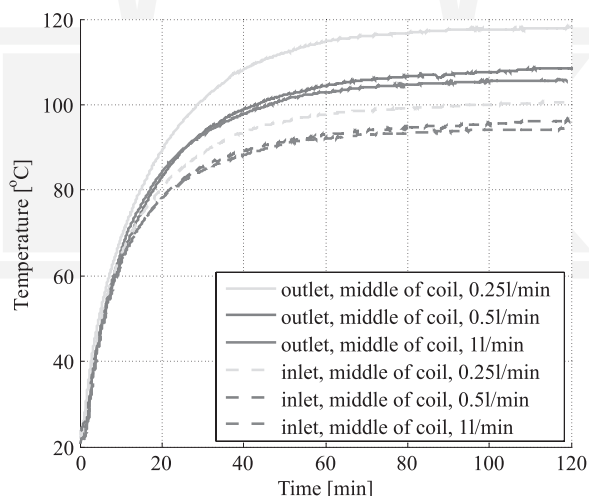


Fig. 9. Maximum temperature of the coil located at the outlet (solid lines) and the coil adjacent to the inlet of the cooling liquid (dashed lines) for different liquid flow rates

Figure 10 shows the dependence of temperature of the liquid flowing in and out of the machine over time. The maximum temperatures are close to the calculated temperatures of hot water from Figs. 5a), 6a) and b). Figures 9 and 10 show that the differences of liquid

temperature are close to the differences of the winding temperature, wherein with increasing speed of liquid, a slight increase in the differences of winding temperatures relative to differences of liquid temperature can be observed.

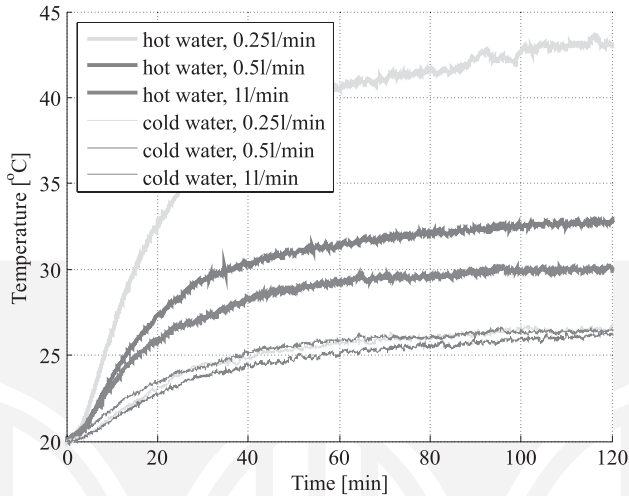


Fig. 10. Temperature of hot and cold liquid at different flow rates

5. Summary

The paper presents a parametric thermal model of the machine with a permanent magnet and external rotor. This model allows determining the temperatures of individual elements of the machine depending on the load and speed of the liquid flow in the cooling channel. The correctness of the model was confirmed by good quantitative correspondence of the calculation results to the test results.

The performed calculation and conducted research suggest that dependence of the maximum winding temperature on the liquid velocity in the channel is highly nonlinear. During determining the optimal liquid flow (as low as possible, which will provide adequate cooling effectiveness), the decreasing power losses in the winding caused by the decreasing temperature and the winding resistance should be compared with the increase in power losses needed to produce the greater liquid flow. In the presented machine, it is the speed approx. 0.5 l/min.

References

- [1] Szczypior J., Jakubowski R., *Konstrukcja maszyny do napędu samochodu elektrycznego o specjalnych wymaganiach*, Prace Naukowe Instytutu Maszyn, Napędów i Pomiarów Elektrycznych Politechniki Wrocławskiej, Nr 66/2012, t. 2, pp. 396–407.

- [2] Szczypior J., Jakubowski R., *Układ chłodzenia i obliczenia cieplne maszyny z magnesami trwałymi i zewnętrznym wirnikiem*, Prace Naukowe Instytutu Maszyn, Napędów i Pomiarów Elektrycznych Politechniki Wrocławskiej, Nr 66/2012, t. 2, pp. 408–417.
- [3] Krok R., *Sieci cieplne w modelowaniu pola temperatury w maszynach elektrycznych prądu przemiennego*, Monografia, Wydawnictwo Politechniki Śląskiej, Gliwice 2010.
- [4] Szczypior J., Jakubowski R., *Obliczenia cieplne w bezrdzeniowej maszynie dyskowej z magnesami trwałymi o chłodzeniu bezpośrednim*, Zeszyty Problemowe – Maszyny Elektryczne, 2009, nr 83, BOBRME Komel, pp. 59–66.
- [5] Szczypior J., Jakubowski R., *Metody bezpośredniego chłodzenia uzwojenia w bezrdzeniowej maszynie dyskowej z magnesami trwałymi*, Zeszyty Problemowe – Maszyny Elektryczne, 2010, nr 88, BOBRME Komel, pp. 109–115.
- [6] Gurazdowski D., Zawilak J., *Rozkład temperatury w pręcie uzwojenia stojana turbogeneratora*, Zeszyty Problemowe – Maszyny Elektryczne, 2006, nr 75, pp. 177–183.
- [7] Domański R., Jaworski M., Kołtyś J., Rebow W., *Wybrane zagadnienia z termodynamiki w ujęciu komputerowym*, PWN, Warszawa 2000.

